POLITECNICO DI TORINO
Repository ISTITUZIONALE

Modeling of the Maximum Induced Currents in Automotive Radiated Immunity Tests via Thevenin-based Metamodels

Original
Modeling of the Maximum Induced Currents in Automotive Radiated Immunity Tests via Thevenin-based Metamodels / Trinchero, R., Stievano, I.S., Canavero, F.. - ELETTRONICO. - (2020), pp. 1-4. (2020 International Symposium on Electromagnetic Compatibility - EMC EUROPE, EMC EUROPE 2020 ita 2020) [10.1109/EMCEUROPE48519.2020.9245759].

Availability:
This version is available at: 11583/2873988 since: 2021-03-12T09:18:57Z

Publisher:
Institute of Electrical and Electronics Engineers Inc.

Published
DOI:10.1109/EMCEUROPE48519.2020.9245759

Terms of use:

This article is made available under terms and conditions as specified in the corresponding bibliographic description in the repository

Publisher copyright
IEEE postprint/Author's Accepted Manuscript

©2020 IEEE. Personal use of this material is permitted. Permission from IEEE must be obtained for all other uses, in any current or future media, including reprinting/republishing this material for advertising or promotional purposes, creating new collecting works, for resale or lists, or reuse of any copyrighted component of this work in other works.

(Article begins on next page)

01 July 2026

Modeling of the Maximum Induced Currents in Automotive Radiated Immunity Tests via Thevenin-based Metamodels

R. Trinchero, I. S. Stievano, and F. G. Canavero
EMC Group, Department of Electronics and Telecommunications, Politecnico di Torino
Corso Duca degli Abruzzi 24, 10129 Torino, Italy
E-mail: riccardo.trinchero@polito.it

***Abstract*—This paper presents three different metamodels for the prediction of the maximum current induced on key vehicle electronic units during an automotive radiated immunity test. The proposed modeling approach is based on a Thevenin circuital interpretation of the test setup which is estimated from a small set of measurements or simulations. The FFT-based trigonometric regression, the support vector machine and the Gaussian process regression are then applied to provide three different metamodels able of predicting the spectrum of the induced currents for any value of the incidence angle of the external EM field. The accuracy and the convergence of the proposed alternatives are investigated by comparing model predictions with the results obtained by means of a parametric full-wave electromagnetic simulation.**

***Index Terms*—Vehicle radiated immunity test, metamodel, Support Vector Machine (SVM) regression, Fast Fourier Transform (FFT), Gaussian Process Regression (GPR), numerical simulation.**

I. Introduction

Metamodels have been widely used in many applications for both optimization purposes and uncertainty quantification, since they provide an efficient and accurate alternative to brute force approaches based on expensive full-computational models. Well-known examples are represented by standard regression and interpolation techniques [1] (e.g., least-squares regression, ridge regression, spline bases, etc..) and machine learning approaches (e.g., Gaussain Process [2], [3], Support Vector Machines [4], [5], Bayesian approaches [6], etc...). The above techniques allow building compact and accurate metamodels of the original system starting from a limited set of responses computed with the full-computational model, usually referred to as training samples.

This work investigates the effectiveness of the metamodels for a specific application belonging to the electromagnetic compatibility (EMC) framework, such as the automotive radiated immunity test [7], [8]. The goal is to develop a metamodel for the above test setup able to predict the spectrum of the maximum current induced on the electronic central unit (ECU) placed inside a vehicle illuminated by a an electromagnetic (EM) field for any value of the azimuth propagation angle. Such model allows a fast assessment of the compliance of the vehicle with the maximum filed levels imposed by the EMC standards [9].

To this aim, a Thevenin-based circuital interpretation [10] of the setup has been developed based on a one-port scattering measurement and a small set of tabulated frequency-domain data obtained from either full-wave simulations or experimental results. Then, a trigonometric regression based on the fast Fourier transform (FFT), the support vector machine (SVM) regression and the Gaussian process regression (GPR) are adopted to build three different models of the voltage source as a function of the incidence angle. The resulting Thevenin-based metamodels allow efficiently predicting the maximum level of the induced currents. A similar idea based on the SVM along with an iterative approach has been recently presented in [8]. This paper investigates the model accuracy of several regression techniques in the extreme case in which the number of training samples is less than 16. The main features and the convergence of the each metamodel are investigated by comparing their predictions with the results of a full-wave simulation with CST Microwave STUDIO.

II. Radiated Immunity Test: Simulation & Thevenin Equivalent

A. Simulation Setup

The radiated immunity test aims at recording the maximum level of the noisy current spectra induced on the main ECUs of a vehicle placed on a rotating floor by an external EM field. The above measurement setup has been implemented in CST Microwave STUDIO. The vehicle under test is modeled as a perfect electric conductor (PEC) structure of dimension $(3.6\times1.55\times2.2)\,\mathrm{m}^3$ with four apertures of dimensions $(0.55\times 1.3)\,\mathrm{m}^2$ and $(0.38\times0.95)\,\mathrm{m}^2$ representing the body of the vehicle and its front and lateral windows [8]. The ECU has been modeled via a lumped load Z_L, which is the far-end termination of a 1-m long transmission line placed inside the vehicle at a fixed heigh of $h = 18\,\mathrm{cm}$ w.r.t. the ground plane. The line is terminated at the near-end with the lumped load $Z_S(\omega)$. The external incident field consists of a plane wave with a vertical polarization for the E-field of amplitude 1 V/m, where the azimuth angle $\phi \in [0, 2\pi[$ to mimic the effect of the rotating floor. The simulation setup allows providing the spectra of the current $I_L(\omega;\phi)$ induced on the transmission line far-end by the incident plane wave for any value of the azimuth angle ϕ in the frequency bandwidth from 1 MHz to 600 MHz via a parametric simulation.

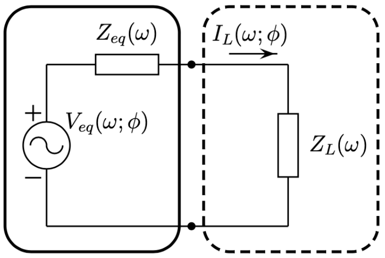

Figure 1: Proposed Thevenin-based circuital interpretation

B. Thevenin-based Equivalent

Within this work, the above test setup has been modeled via the Thevenin equivalent shown in Fig. 1. The Thevenin equivalent is estimated from two different sets of measured or simulated data. First of all, the equivalent impedance of the structure is estimated via a one-port scattering characterization, where the $S_{11}(\omega)$ parameter is measured or simulated at the ECU port (i.e., the far-end of the transmission line) for a fixed impedance $Z_S(\omega)$ and without the incidence field. The equivalent impedance $Z_{eq}(\omega)$ is then calculated as:

$$Z_{eq}(\omega) = \frac{1 + S_{11}(\omega)}{1 - S_{11}(\omega)} 50\Omega. \tag{1}$$

for any angular frequency ω within the frequency bandwidth of the simulation.

Once the equivalent impedance Z_{eq} has been calculated via (1), the equivalent Thevenin source $\bar{V}_{eq}(\omega;\phi_i)$ can be suitably estimated from the spectra $I_{L0}(\omega;\phi_i)$ of the current induced on a known load Z_{L0} for a given set of angles ϕ_i with $i = 1,\ldots,N$, as follows:

$$\bar{V}_{eq}(\omega;\phi_i) = I_{L0}(\omega;\phi_i)(Z_{eq}(\omega) + Z_{L0}(\omega)). \tag{2}$$

Finally, the obtained Thevenin equivalent allows estimating the current $I_L(\omega,\phi_i)$ induced on a generic load $Z_L(\omega)$, representing the input port of the ECU, for a given set of angles ϕ_i [8]:

$$I_L(\omega,\phi_i) = \frac{\bar{V}_{eq}(\omega,\phi_i)}{Z_{eq}(\omega) + Z_L(\omega)}. \tag{3}$$

III. Metamodel of V_{eq}

The Thevenin equivalent presented in the previous Section allows predicting the spectrum of the noisy current $I_L(\omega,\phi_i)$ induced on a generic load Z_L for a discrete set of incidence angles $\{\phi_i\}_{i=1}^N$. Indeed, $\bar{V}_{eq}(\omega;\phi_i)$ is known only for the discrete set of angular values ϕ_i used in (2). Regression techniques can be used to overcome the above limitation, leading to a metamodel able to approximate the real and imaginary parts of the voltage $V_{eq}(\omega;\phi)$ for any value of the incidence angle $\phi \in [0, 2\pi[$. Three different regression techniques are considered. For the sake of notation simplicity, in the following formulation we consider the simplified case in which $V_{eq}(\omega;\phi) \in \mathbb{R}$. However, in the actual implementation, two different regressions have been trained in parallel by considering the real and the imaginary part of the available samples of $\bar{V}_{eq}(\omega;\phi_i)$.

A. FFT-based Trigonometric Regression

A trigonometric regression can be considered as the most straightforward way to account for the periodic behavior of the source $V_{eq}(\omega;\phi)$ with respect to the angle ϕ (e.g, $V_{eq}(\omega;0) = V_{eq}(\omega;2\pi)$) [10]. For a given angular frequency ω_0, the regression writes:

$$V_{eq,\text{FFT}}(\omega_0;\phi) = \sum_{n=-\lfloor N/2 \rfloor}^{-\lfloor N/2 \rfloor} V_{eq,n}(\omega_0) \exp(jn\phi), \tag{4}$$

where the coefficients $V_{eq,n}$ can be efficiently computed by applying the FFT algorithm on the training samples $\bar{V}_{eq}(\omega_0;\phi_i)$ for $i = 1,\ldots,N$, since the angles $\{\phi_i\}_{i=1}^N$ are uniformly spaced. Such procedure can be easily extended to the case of non-uniform spaced samples via a least-squares formulation.

B. Support Vector Machine (SVM) Regression

The SVM regression can be adopted to provide a periodic metamodel for the source $V_{eq}(\omega;\phi)$. For a given angular frequency ω_0, the SVM regression in the dual-space writes [4]:

$$V_{eq,\text{SVM}}(\omega_0;\phi) = \sum_{i=1}^{N} \beta_i(\omega_0) K(\phi_i,\phi) + b(\omega_0), \tag{5}$$

where $\beta_i(\omega_0)$ and $b(\omega_0)$ are the frequency-dependent coefficients and bias term, respectively. Such regression unknowns are computed by solving a quadratic optimization problem which involves the minimization of the so-called ε-intensive loss function [4].

For this specific application, the kernel $K(\phi_i,\phi)$ has been defined via the periodic regularized Fourier expansion [4]), which writes:

$$K(\phi_i,\phi) = \frac{1 - q^2}{2(1 - 2q\cos(\phi_i - \phi) + q^2)} \text{ for } 0 < q \leq 1. \tag{6}$$

It is important to remark, that different from a plain least-squares regression, the optimization behind the SVM regression do not only minimize the ε-intensive loss function, but it also tries to keep the values of the coefficients β_i as lower as possible, thus avoiding overfitting.

C. Gaussian Process Regression (GPR)

The GPR can be used to provide the user with a probabilistic model. At a given angular frequency ω_0, the actual value of the voltage source $V_{eq}(\omega_0;\phi)$ can be approximated in terms of the following Gaussian precess [2]:

$$V_{eq}(\omega_0;\phi) \approx \mathcal{GP}_{\omega_0}(0, k(\phi,\phi')), \tag{7}$$

with zero mean and covariance function $k(\phi', \phi)$. The latter provides the correlation between the value of V_{eq} at ϕ and ϕ'. Also, in this case a periodic covariance function is used:

$$k(\phi, \phi') = \sigma^2 \exp\left(-\frac{2}{l^2}\sin^2\left(\pi|\phi - \phi'|\right)\right), \tag{8}$$

where σ and l are the hyper-parameters associated to the covariance function.

Different from the regressions in (4) and (5), the GPR in (7) provides for any value $\phi_* \in [0, 2\pi[$ a probabilistic interpretation of the value $V_{eq}(\omega_0; \phi_*)$ in terms of a Gaussian probability distribution:

$$V_{eq,\text{GPR}}(\omega_0; \phi) \sim \mathcal{N}(\mu_{\phi_*}(\omega_0), \sigma^2_{\phi_*}(\omega_0)) \tag{9}$$

where the mean $\mu_{\phi_*}(\omega_0)$ and the variance $\sigma^2_{\phi_*}(\omega_0)$ are computed from the available training samples and the covariance $k(\cdot, \cdot)$ (see [2] for additional details).

The above probabilistic formulation of the model output allows predicting the upper and lower bounds of the confidence interval (CI), such that given the available information on the training samples, the actual value of $V_{eq}(\omega_0; \phi)$ writes:

$$V_{eq}(\omega_0; \phi) \in \\ [\mu_{\phi_*}(\omega_0) - z_{1\text{-}\frac{\alpha}{2}}\sigma_{\phi_*}(\omega_0), \mu_{\phi_*}(\omega_0) + z_{1\text{-}\frac{\alpha}{2}}\sigma_{\phi_*}(\omega_0)] \tag{10}$$

with a probability of $100(1-\alpha)\%$, where z denotes the inverse of the Gaussian cumulative distribution function evaluated at $1 - \frac{\alpha}{2}$. The bounds of the $V_{eq,\text{GPR}}$ defined by CIs can be propagated through the corresponding bounds of the induced current via (3) by using the interval arithmetic [11].

IV. Validation

The effectiveness of the three metamodels presented in the previous sections is investigated by considering the current spectra $I_L(\omega; \phi)$ induced by an external EM field with azimuth angle $\phi \in [0, 2\pi[$ for the case of a reactive ECU load $Z_L(\omega) = R_L + j\omega L_L + 1/j\omega C_L$ where $R_L = 10\,\Omega$, $L_L = 0.1\mu$H and $C_L = 0.1$ nF, and with $Z_S = 1\,\text{k}\Omega$.

The parameters of the Thevenin equivalent in Fig. 1, have been calculated from (1) and (2) by considering the scattering parameter and the current samples $I_{L0}(\omega; \phi_i)$ provided by the full-wave solver of CST Microwave STUDIO via the simulation setup described in Sec. II.1, with $Z_{L0} = 50\,\Omega \neq Z_L(\omega)$. The accuracy and the convergence of each of the three metamodels are investigated for an increasing number of training samples $N = 7$ and 15 (i.e., the number of current spectra used to train the metamodels).

As a fist validation, Fig. 2 shows a comparison among the current magnitude $I_L(2\pi f_0; \phi)$ for $f_0 = 403$ MHz obtained via the results of a parametric CST simulation for 150 different values of the incidence angle ϕ_i with the ones predicted by the metamodels based on the trigonometric regression, SVM regression and the 99% CI predicted by the GPR built with few samples (i.e., with $N = 7$ and 15 training samples). The results obtained with $N = 7$ highlight the importance of the CIs provided by combining the GPR with the interval analysis. Indeed, even if the number of training samples is not enough to get an accurate model, the CIs (green area) predicted by the GPR provide a conservative estimation of the actual maximum level of the current $I_L(2\pi f_0; \phi)$ with respect to the angle ϕ. On the other hand, for $N = 15$, the CIs become smaller and the results of the three metamodels are almost equivalent.

Table I: Comparison among the RMSE computed by comparing the results of a full-wave parametric simulation with 150 angular samples and the corresponding ones predicted by the proposed metamodels built with a limited number of training samples ($N = 7$ and $N = 15$).

Method	RMSE $N = 7$	RMSE $N = 15$
FFT	7.0189×10^{-4}	4.4483×10^{-4}
SVM	6.6096×10^{-4}	4.3280×10^{-4}
GPR	6.5782×10^{-4}	4.3958×10^{-4}

As a final validation, Fig. 3 compares frequency by frequency the values of the maximum level and the mean values of the current $I_L(\omega; \phi)$ estimated by the three models with 150 CST simulations in the bandwidth 1 MHz to 600 MHz. Also in this case, the results show the capability of the CI computed with the GPR of providing a conservative estimation of the actual maximum value of the current spectra $I_L(\omega; \phi)$, when only $N = 7$ training sample are available (see the green area). However, again the three methods are almost equivalent for $N = 15$. In the above results, $q = 0.5$ in the SVM kernel of (6) and the hyper-parameters for the covariance function in (8) take the following values: $\sigma = 1$, $l = 5.5$ for $N = 7$ and $\sigma = 3.5$, $l = 1$ for $N = 15$.

A more detailed overview on the model accuracy is given in Tab. I in terms of their root-mean-squared error (RMSE). The error values show that the metamodel based on the GPR is the most accurate for $N = 7$, and that the SVM metamodel is the most accurate for $N = 15$, but in both cases the accuracy provided by the two models are very close each other. Summarizing, the three metamodels can be considered as good candidates for the prediction of the maximum currents induced during a radiated immunity vehicle test. However, the one based on GPR seems providing the best results in the extreme case when few training sample are available (i.e., less than 10).

V. Conclusions

This paper deals with the development of an accurate and efficient metamodel for the prediction of the maximum current spectra induced in a radiated immunity vehicle test via a Thevenin-based circuital intrepretation. Such circuital interpretation, estimated from two sets of measured or simulated data, is then combined with three different regression techniques to get a metamodel able of approximating the current values for

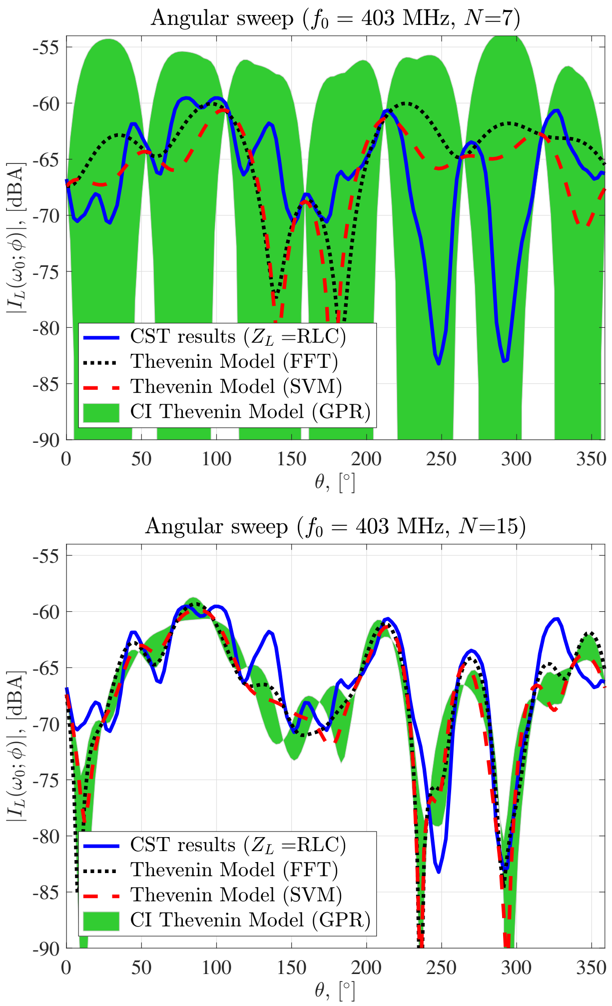

Figure 2: Magnitude of the current $I_L(2\pi f_0;\phi)$ for $f_0 = 403$ MHz as a function of the angle ϕ. The reference responses obtained via a parametric full-wave simulation with 150 angular samples are superimposed with the corresponding values predicted by the proposed metamodels built with $N = 7$ (top panel) and 15 (bottom panel) training samples.

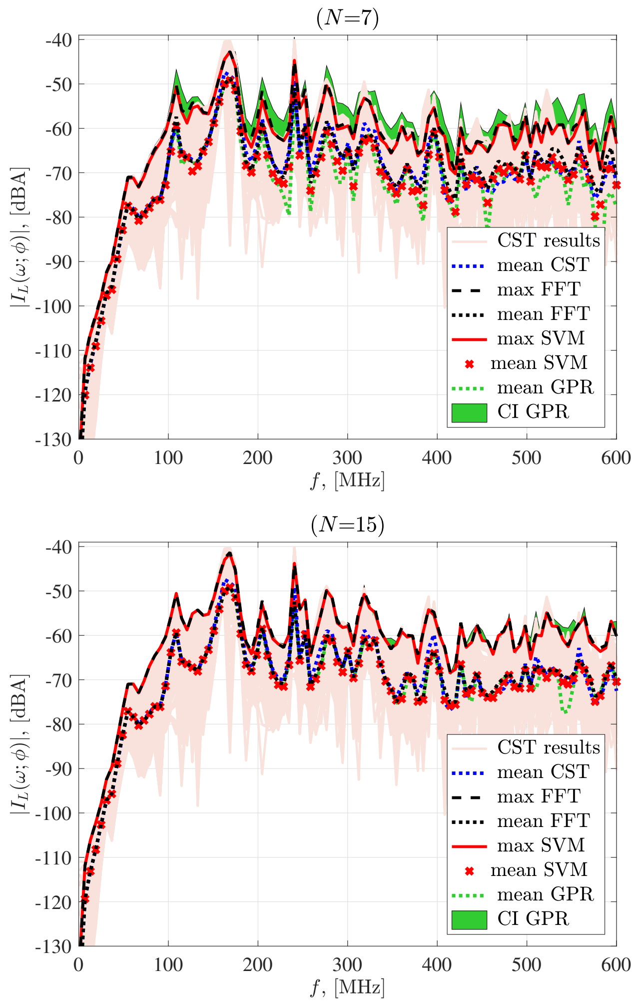

Figure 3: Maximum spectrum of the current $I_L(\omega;\phi)$. The reference responses obtained via a parametric full-wave simulations are compared with the maximum and mean values predicted by the proposed metamodels built with $N = 7$ (top panel) and 15 (bottom panel) training samples.

any value of the azimuth angle of the incident EM field.

The accuracy and the robustness of the considered regression techniques has been investigated by comparing their prediction with the reference results provided by a parametric full-wave simulation. According to the results, the metamodel based on the GPR seems to be the most reliable one when only few training samples are available.

References

[1] K. T. Fang, R. Li, A. Sudjianto, “Design and modeling for computer experiments”, Taylor & Francis Group, LLC, London, 2016.

[2] C. E. Rasmussen and C. K. I. Williams, *Gaussian Processes for Machine Learning*, MIT Press. Cambridge, Massachusetts, 2006.

[3] R. Trinchero and F. G. Canavero, “Machine Learning for the Design of a Distribution Network for High-Speed Signals,” in *International Conference on Electromagn. in Advanced Applications*, Granada, Spain, 2019, pp. 1038-1041.

[4] V. Vapnik, *Statistical Learning Theory*, John Wiley and Sons, NY, 1998.

[5] R. Trinchero, P. Manfredi, I. S. Stievano and F. G. Canavero, “Machine Learning for the Performance Assessment of High-Speed Links”, *Trans. Electromagn. Compat.*, vol. 60, no. 6, pp. 1627-1634, Dec. 2018.

[6] S. De Ridder, *et al.*, "A Bayesian Approach to Adaptive Frequency Sampling," in *IEEE Workshop on Sign. and Power Int.*, Chambéry, France, 2019, pp. 1-4.

[7] A. M. Silaghi, *et al.*, “Measurement of radiated immunity in the automotive industry: Key concepts,” in *Proc. IEEE 12th Int. Symp. on Electronics and Telecommunications*, Timisoara, 2016, pp. 25–28.

[8] R. Trinchero, I. S. Stievano and F. G. Canavero, “Black-Box Modeling of the Maximum Currents Induced in Harnesses During Automotive Radiated Immunity Tests,” *IEEE Trans. Electromagn. Compat.*, vol. 62, no. 2, pp. 627–630, April 2020.

[9] Road Vehicles & Component Test Methods for Electrical Disturbances From Narrowband Radiated Electromagnetic Energy–Part 4: Harness Excitation Methods, ISO 11452-4, Dec. 2011.

[10] S. Grivet-Talocia and E. Fevola, “Compact Parameterized Black-Box Modeling via Fourier-Rational Approximations,” *IEEE Trans. Electromagn. Compat.*, Vol. 59, No. 4, pp. 1133–1142, Aug. 2017.

[11] T. Ding, *et al.*, “How Affine Arithmetic Helps Beat Uncertainties in Electrical Systems,” *IEEE Circuits Syst. Mag.*, vol. 15, no. 4, pp. 70–79, Nov. 2015.